Limit equilibrium analysis of masonry buttresses and towers under lateral and gravity loads

Nicos Makris & Haris Alexakis

Archive of Applied Mechanics

ISSN 0939-1533

Arch Appl Mech
DOI 10.1007/s00419-015-1027-2



Springer

Your article is protected by copyright and all rights are held exclusively by Springer-Verlag Berlin Heidelberg. This e-offprint is for personal use only and shall not be self-archived in electronic repositories. If you wish to self-archive your article, please use the accepted manuscript version for posting on your own website. You may further deposit the accepted manuscript version in any repository, provided it is only made publicly available 12 months after official publication or later and provided acknowledgement is given to the original source of publication and a link is inserted to the published article on Springer's website. The link must be accompanied by the following text: "The final publication is available at link.springer.com".



Author's personal copy

Arch Appl Mech
DOI 10.1007/s00419-015-1027-2

ORIGINAL

Nicos Makris · Haris Alexakis

Limit equilibrium analysis of masonry buttresses and towers under lateral and gravity loads

Received: 7 April 2015 / Accepted: 30 May 2015
© Springer-Verlag Berlin Heidelberg 2015

Abstract This paper revisits the fracturing of masonry buttresses and towers when subjected either to a concentrated oblique force at their head or to lateral inertial loading due to ground shaking and presents the corresponding failure criteria in elongation and shear. The loading configurations examined result either from the thrust that an elevated arch exerts on its supporting buttresses or from earthquake shaking on solitary masonry towers. At their limit state, tall, slender masonry buttresses and towers collapse by pivoting about their base corner, whereas less slender masonry structures may collapse by developing a shear failure. Because of the unilateral behavior of masonry, at the initiation of collapse of a slender buttress, the compression-free region separates from the rest of the buttress and reduces the stabilizing moment. As the ratio, base/height or the gravity load, increases, masonry buttresses and towers may fail in shear; therefore, the paper presents envelopes of their limit lateral capacity depending on the aspect ratio, the mechanical properties of masonry and the level of vertical loading. The equivalent static analysis adopted in this paper concludes that in most cases under lateral inertial loading, elongation failure is the lower failure mechanism of a tall masonry tower; nevertheless, a subsequent initiation of rocking that engages the large rotational inertia of the detached portion of the tower attracts additional inertia forces that may induce a follower shear failure.

Keywords Stone towers · Seismic analysis · Limit state · Hinging mechanism · Shear failure · Historic structures

1 Introduction

Masonry arches exert inclined thrust forces at their springings. In the event that the arch is an elevated structure supported upon buttresses, the inclined thrust force at the springing of the arch is loading the buttresses as shown in Fig. 1. Clearly, the failure of a buttress leads to a catastrophic collapse; therefore, its appropriate sizing has been a concern throughout the history of masonry structures ([1–8] among others). Figure 2 shows

N. Makris (✉)
Division of Structures, Department of Civil, Environmental and Construction Engineering, University of Central Florida, Orlando, FL 32816, USA
E-mail: Nicos.Makris@ucf.edu

N. Makris
Office of Theoretical and Applied Mechanics, Academy of Athens, 10679 Athens, Greece

H. Alexakis
Division of Structures, Department of Civil Engineering, University of Patras, 26500 Patras, Greece
E-mail: alexakis@upatras.gr

Published online: 12 June 2015

Author's personal copy

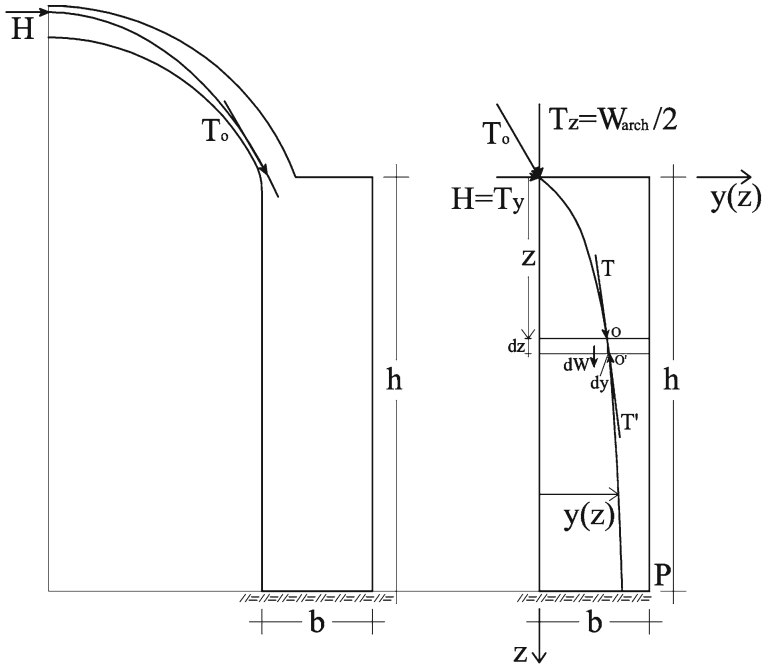


Fig. 1 *Left* Schematic of a masonry arch supported on vertical masonry buttresses. The thrust forces from the arch are transferred to the masonry buttresses as inclined forces at their heads. *Right* Thrust line along the buttress subjected to the inclined thrust force, T_o, at its head and to its weight



Fig. 2 Masonry arches atop buttresses at the façade of the Odeon of Herodes Atticus in Athens, Greece

Author's personal copy

a photograph from part of the façade of the Odeon of Herodes Atticus in Athens, Greece, where masonry buttresses are supporting arches atop.

Under a sufficiently large inclined force, a tall slender buttress will fail as it tends to pivot about its extrados corner P at its base, while at the same time, its compression-free portion separates from the failing buttress. On the other hand, a less slender buttress with relatively low cohesion along the stone joints will fail in shear when subjected to a sufficiently large inclined force. The elongation and shear failure mechanism are also the two plausible failure mechanisms of a solitary masonry tower subjected to earthquake shaking.

This paper builds on earlier work on the elongation failure of slender towers and buttresses [9,10] and revisits the limit equilibrium analysis of masonry buttresses and towers by also accounting for a plausible shear failure. This study presents failure envelops for the masonry buttress that has zero tensile strength, sufficient compression strength and finite shear strength.

2 Thrust line of a masonry buttress under an inclined load at its head

Before examining the fracturing pattern of a masonry buttress under an inclined static load at its head, it is worth revisiting the equation of the thrust line that prevails in the buttress prior to fracture. Figure 1 shows a symmetric structure subjected to symmetric loading; therefore, we concentrate on the right buttress of width, b, and height, h, where the thrust line $y(z)$ initiates at the origin of the axis ($z = 0,\ y = 0$) and evolves with a positive slope. The thrust line $y(z)$ is the geometrical locus of the application points of the resultant thrust force acting at any horizontal cross section of the buttress. In reality, a masonry buttress is not a monolithic column since it consists of individual stones built and wedged together with or without mortar. Nevertheless, in most cases the stones are placed roughly in horizontal courses; therefore, the assumption of a horizontal stereotomy is reasonable [11–17].

With reference to Fig. 1, let T_o be the resultant thrust force at the upper-left corner of the right buttress having a horizontal component, T_y, and a vertical component T_z. At a distance, z, from the upper-left corner, that is the origin of the system of axis z, y, the thrust force is T, while at a distance $z + dz$, the thrust force is $T^{'}$ and its application point is $O^{'}$. Moment equilibrium of the elementary slice of the buttress bdz about point $O^{'}$ gives:

$$(T_z + \gamma bz)\, dy = T_y dz + dW\left(\frac{b}{2} - y(z) - dy\right) \tag{1}$$

where $dW = \gamma b dz$ and γ is the surface force density of the buttress ([Force]/[Length]^2). After eliminating higher-order differentials, Eq. (1) gives

$$(z + t_z h)\,\frac{\mathrm{d}y(z)}{\mathrm{d}z} + y(z) = t_y h + \frac{b}{2} \tag{2}$$

where $t_y = T_y/(\gamma bh)$ and $t_z = T_z/(\gamma bh)$ are the normalized horizontal and vertical forces acting at the head of the buttress to the weight of the entire buttress $= \gamma bh$.

The solution of the linear differential Eq. (2) is

$$y(z) = \frac{A}{z + t_z h} + t_y h + \frac{b}{2} \tag{3}$$

where A is an integration constant which shall satisfy the boundary condition $y(z = 0) = 0$. Accordingly, $A = -t_y t_z h^2 - t_z h(b/2)$, and Eq. (3) becomes

$$y(z) = h\left(\frac{1}{2}\frac{z}{h}\frac{s + 2t_y}{\frac{z}{h} + t_z}\right) \tag{4}$$

where $s = b/h$ is the slenderness of the buttress. In terms of the normalized ordinate of the thrust line $\bar{y}(z) = \frac{y(z)}{b}$ $(0 \le \bar{y}(z) \le 1)$, Eq. (4) yields

$$\bar{y}(z) = \frac{y(z)}{b} = \frac{1}{2s}\frac{z}{h}\frac{s + 2t_y}{\frac{z}{h} + t_z} \tag{5}$$

Author's personal copy

As the ratio of the horizontal to the vertical load increases, the thrust line tends to the exterior point P at the base of the buttress. In the event that the buttress maintains its integrity and tends to pivot about the exterior point P as a monolithic structure (no fracturing—[18–21]), the limit state of the buttress is reached when the thrust line given by Eqs. (4) or (5) passes by point P—that is $y(z = h) = b$ (or $\bar{y}(z = h) = 1$). Accordingly, at this limit state (pivoting without fracturing), Eq. (5) gives that the critical horizontal normalized force $t_y = T_y/(\gamma bh)$ at the head of the buttress is given by

$$t_y = \frac{T_y}{\gamma bh} = s\left(\frac{1}{2} + t_z\right) \tag{6}$$

For instance, for the special case of a monolithic buttress loaded by only a horizontal force at height h ($t_z = 0$), Eq. (6) yields that $t_y = \frac{T_y}{\gamma bh} = \frac{s}{2} = \frac{1}{2}\frac{b}{h}$, which is the result that one recovers from simple moment equilibrium about point P.

3 Elongation failure of a slender masonry buttress under an inclined load at its head

In reality, a masonry buttress consists of individual stones and only compressive forces can be transmitted across its joints. Consequently, any tendency for elongation in the buttress separates the stones in the compression-free region and eventually results to an inclined fracture.

With reference to Fig. 3, the initiation of the compression-free region of the buttress can be easily computed with Eq. (4) after assuming a triangular stress distribution. In this case, the compression-free region originates at a distance z_e from the axis origin where the base of the triangular stress distribution is equal to the width of the buttress, b. Accordingly, at this distance z_e, the resultant thrust force T_e will be at a distance $y(z) = 2b/3$. By setting the left-hand side of Eq. (4) equal to $2b/3$, one obtains

$$\frac{z_e}{h} = \frac{4st_z}{6t_y - s} \tag{7}$$

The result offered by Eq. (7) has been also presented by Ochsendorf et al. [10] after taking moment equilibrium of the upper portion of the buttress about point M (the application point of T) that is at a distance $= 2b/3$ away from the intrados side of the buttress.

The motivation for investigating the fracturing of a buttress when subjected to an oblique static load emerges from the need to estimate the stabilizing moment that is due to only a portion of its weight, since the detached, compression-free portion of the buttress does not participate in the imminent mechanism of collapse. This problem was investigated about a decade ago by Ochsendorf et al. [10], Ochsendorf and De Lorenzis [22] who concluded that the line of fracture of a rectangular masonry buttress is straight. While the straight-line fracture presented by Ochsendorf et al. [10] is correct, their mathematical derivation [equation (2) to (7) in their 2004 paper] is rather obscure. According to figure 4 presented in the Ochsendorf et al. [10] paper, their independent variable is y (that is their vertical axis), the elementary slice of the buttress involved in the differential calculus has thickness dy, and their formulation sets the stage for the search of the unknown fracture line $x(y)$. Interestingly, their derivation concludes with the equation $\mathrm{d}^2y/\mathrm{d}x^2 = 0$ which suffers from the lack of boundary conditions given that during their derivation, the dependent and independent variables have been interchanged. The alternative vertical fracture line given by equation (8) in the Ochsendorf et al. [10] paper is expressed as $x(y) =$ constant, and the role of dependent and independent variables is again reversed.

In our analysis (see Fig. 3), the vertical axis $= z$ (z $=$independent variable), and we are in search of the line of fracture $f(z)$. Assuming a triangular vertical stress distribution, the line of fracture $f(z)$ is the geometrical locus of the points in the buttress where the vertical compressive stresses vanish. Accordingly, at any location z of the fractured portion of the buttress, the resultant of the vertical forces, $W = W(z)$, is at a distance $(b - f(z))/3$ from the side of the buttress that passes by the imminent pivot point, P. With reference to Fig. 3, moment equilibrium of the upper portion of the buttress about point K gives

$$W(z)\frac{b - f(z)}{3} + dW(z)\frac{b - f(z) - \frac{df(z)}{2}}{2} = (W(z) + dW(z))\frac{b - f(z) - df(z)}{3} + T_y dz \tag{8}$$

After eliminating higher-order differentials, Eq. (8) gives

$$W(z)\frac{\mathrm{d}f(z)}{\mathrm{d}z} = 3T_y - \frac{1}{2}(b - f(z))\frac{\mathrm{d}W(z)}{\mathrm{d}z} \tag{9}$$

Author's personal copy

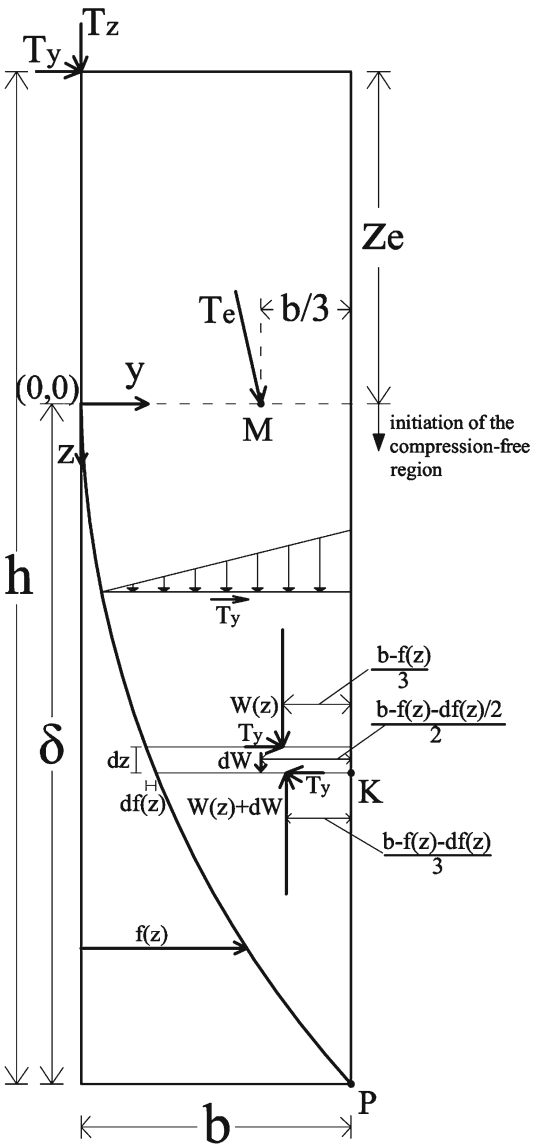


Fig. 3 Elongation failure of a masonry buttress with surface density, γ, along the unknown curve $f(z)$ due to an inclined force at its head with magnitude $\sqrt{T_y^2 + T_z^2}$

At the same time, the weight of a horizontal slice of the ruptured buttress is $dW(z) = \gamma(b - f(z))dz$; therefore,

$$\frac{\mathrm{d}W(z)}{\mathrm{d}z} = \gamma\,(b - f(z)) \tag{10}$$

where γ is the surface force density of the buttress.

Substitution of Eq. (10) into (9) gives

$$W(z)\frac{\mathrm{d}f(z)}{\mathrm{d}z} = 3T_y - \frac{1}{2}\gamma\,(b - f(z))^2 \tag{11}$$

Equation (11) can be expressed as

$$W(z) = \left(\frac{\mathrm{d}f(z)}{\mathrm{d}z}\right)^{-1}\left(3T_y - \frac{1}{2}\gamma\,(b - f(z))^2\right) \tag{12}$$

Author's personal copy

and upon differentiation,

$$\frac{\mathrm{d}W(z)}{\mathrm{d}z} = -\frac{\mathrm{d}^2 f(z)}{\mathrm{d}z^2}\frac{1}{\left(\frac{\mathrm{d}f(z)}{\mathrm{d}z}\right)^2}\left(3T_y - \frac{1}{2}\gamma\,(b - f(z))^2\right) + \gamma\,(b - f(z)) \tag{13}$$

Equation (13) assumes the following form after making use of Eq. (10)

$$\frac{\mathrm{d}^2 f(z)}{\mathrm{d}z^2}\left(3t_y - \frac{1}{2}s\left(1 - \frac{f(z)}{b}\right)^2\right) = 0 \tag{14}$$

where $t_y = T_y/(\gamma bh)$ is the normalized horizontal force at the head of the buttress to the weight of the entire buttress $= \gamma bh$.

Equation (14) is satisfied either when the term in the parenthesis equals to zero or when $\mathrm{d}^2 f(z)/\mathrm{d}z^2 = 0$. When the term in the parenthesis is set equal to zero, the resulting fracture line is $f(z) = b\left(1 \pm \sqrt{6t_y/s}\right)$— that is a vertical line along the entire height of the buttress. The root with the positive sign before the radical is rejected since the thrust line needs to be within the geometry of the buttress. The root with the negative sign before the radical is also rejected given that according to the assumptions of this analysis, the upper portion of the buttress (from the abscissa $z_e = 4hst_z/(6t_y - s)$ and above) has no reason to fracture since the entire width of the buttress is in compression. Accordingly, the only admissible solution from Eq. (14) is that $\mathrm{d}^2 f(z)/\mathrm{d}z^2 = 0$ which upon integration gives

$$f(z) = A_1 z + A_2 \tag{15}$$

In Eq. (15), A_1 and A_2 are integration constants to be determined from the boundary conditions. In this analysis, the origin of the system of axis is translated down at $z = z_e$, so that the fracture initiates at $z = 0$. Furthermore, in this analysis we are in search of the fracture line $f(z)$ of a slender buttress which collapses by pivoting about the base corner P, when the horizontal thrust force $T_y = t_y \gamma bh$ is sufficiently large. Consequently, when the collapse mechanism is imminent, the line of fracture $f(z)$ will pass by the pivoting point, P; therefore, the boundary conditions of Eq. (15) are as follows: $f(0) = 0$ and $f(\delta) = b$, where $\delta = h - z_e$. By enforcing these boundary condition, $A_2 = 0$ and $A_1 = b/\delta$, and Eq. (15) gives

$$f(z) = s\frac{6t_y - s}{6t_y - s\,(1 + 4t_z)}z \tag{16}$$

Equation (16) offers the line of fracture of a masonry buttress which originates at a distance $z_e = 4hst_z/(6t_y - s)$ below the head of the buttress and propagates linearly to meet the extrados pivot point P at the base of the buttress. The linear fracture given by Eq. (16) materializes when the horizontal thrust t_y is sufficiently large for any given value of the vertical force t_z. At the limit equilibrium state, the critical value of t_y is computed by taking moment equilibrium about the imminent pivot point P. Knowing that the fracture line is linear [see Eq. (16)], moment equilibrium about point P gives:

$$t_y = s\left(t_z + \frac{1}{2} - \frac{1}{3}r\right) \tag{17}$$

where $r = \delta/h$ is the fracture ratio given by

$$r = \frac{\delta}{h} = \frac{h - z_e}{h} = 1 - \frac{4st_z}{6t_y - s} \tag{18}$$

Substitution of Eq. (18) into Eq. (17) yields a quadratic equation, and its solution gives the value of the critical normalized horizontal thrust $t_y = T_y/(\gamma bh)$ for any given value of the vertical thrust $t_z = T_z/(\gamma bh)$.

$$t_y = \frac{s}{6}\left(1 + 3t_z + \sqrt{9t_z^2 + 8t_z}\right) \tag{19}$$

Equation (19) is a statement of the failure criterion of a buttress that fails in elongation. It is a failure criterion that does not contain any material parameters given that the analysis assumes that the joints of the masonry have zero tensile strength. Figure 4 plots the value of the critical horizontal thrust, t_y, offered by Eq. (19) as the normalized vertical force increases and compares it with the corresponding overturning horizontal thrust given by Eq. (6) which is for a monolithic buttress that does not fracture.

Author's personal copy

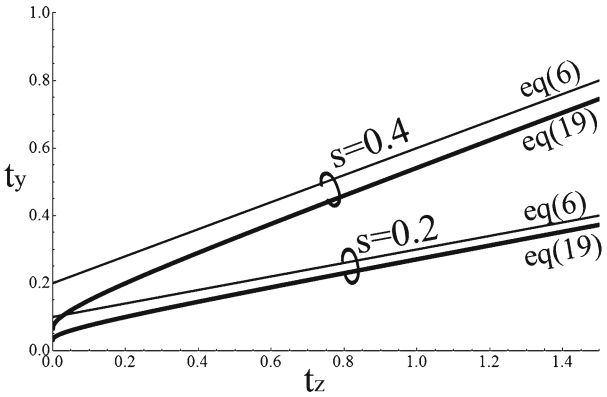


Fig. 4 Critical normalized horizontal force $t_y = T_y/(\gamma bh)$ at the head of a buttress with slenderness, s, that is needed to create an elongation failure as a function of the normalized vertical force $t_z = T_z/(\gamma bh)$ at the buttress head

4 Are vertical buttresses with zero tensile strength physically realizable?

Figure 5 (top) shows a column under compression that is built out of some material that has sufficient compression strength. An infinitesimal element of the column that is along the vertical boundary is subjected to a finite vertical stress, σ_V; while the horizontal stress is zero ($\sigma_H = 0$). Assuming that the material element is close to a stress-free boundary, the stresses σ_V and σ_H are principal. Figure 5 (bottom) shows the Mohr circle that corresponds to the stress state (σ_V, σ_H). As σ_V increases, the Mohr circle grows and eventually reaches some failure boundary. Given that $\sigma_H = 0$ is zero, the failure boundary that is tangent to the critical circle shall cross the vertical axis, τ, at some finite distance, c, from the axis origin. This finite shear strength, c, that is available at zero normal stress is the cohesion of the material. Consequently, Figure 5 indicates that in order for a vertical monolithic column to sustain a compression load, its material needs to exhibit a finite cohesion, c. Figure 5 (bottom) also indicates that regardless how sharply the failure boundary bends to meet the horizontal stress axis, σ, it always encloses a finite tensile stress, σ_e, indicating that for a vertical monolithic column to sustain a compression load, its material needs to exhibit some finite tensile strength $= \sigma_e$.

A masonry buttress is not a monolithic column, since it consists of individual stones placed roughly in horizontal courses and laid with or without mortar between the stones. From the previous discussion, it is clear that any individual stone (in particular those which are along the side of the buttress) need to exhibit some finite tensile strength in order for the buttress to remain standing under axial compression. Nevertheless, the joints in-between the individual stones may have a minimum or even zero tensile strength; therefore, the rupture at the limit equilibrium state may develop by following a critical path along the joints of the stones as shown schematically in Fig. 5 (right). Consequently, the assumption of a buttress with zero tensile strength is physically realizable as long as the fracture happens along the joints of the stones which do not sustain tension. Figure 5 indicates that the theoretical fracture line given by Eq. (16) has practical significance when the size of the stones is sufficiently small. At the same time, the stone blocks need to be large enough to ensure stability of the buttress. For instance, it is not possible to build a tall, slender, load bearing buttress out of very small stone blocks—say the size of a dice, given that such a masonry structure will fail due to instability effects [9].

5 Shear failure of a stocky masonry buttress under an inclined load at its head

While the joints of the individual stones in masonry structures have negligible tensile strength, they exhibit finite shear strength because of the friction and occasional larger-scale macroscopic interlocking that develops along the interface of stones with finite size. In this analysis, we assume a simple Coulomb law for the friction force, F, that develops along the sliding interface [23],

$$F = \mu N + Cl \tag{20}$$

where μ is the coefficient of friction, N is the resultant force normal to the sliding interface, C is the cohesion force per length and l is the length of the shearing plane.

Author's personal copy

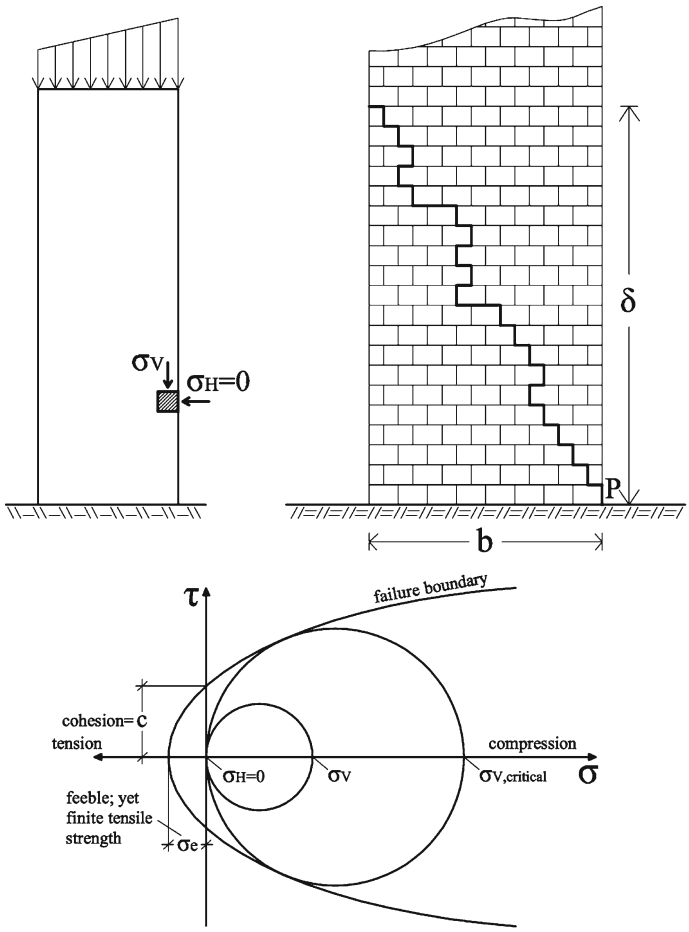


Fig. 5 For a masonry buttress to sustain a compression load, each building block needs to exhibit some finite cohesion together with some finite tensile strength, whereas the joints of the buttress may exhibit zero tensile strength. Consequently, the assumption of a buttress with zero tensile strength is physically realizable

With reference to Fig. 6, we analyze the situation where the masonry buttress fails in shear along a plane that is inclined at an angle φ. Denoting by z_s the distance from the head of the buttress where the failure plane initiates, the weight of the upper portion of the buttress is

$$W_1 = \gamma bh\left(\frac{z_s}{h} + \frac{s}{2}\tan\phi\right) \tag{21}$$

Macroscopic force equilibrium parallel and normal to the failure plane gives

$$(T_z + W_1)\sin\phi + T_y\cos\phi = \mu N + C\frac{b}{\cos\phi} \tag{22}$$

$$N = (T_z + W_1)\cos\phi - T_y\sin\phi \tag{23}$$

The combination of Eqs. (21), (22) and (23) gives the normalized horizontal critical force, $t_y = T_y/(\gamma bh)$, capable of initiating sliding

$$t_y = \frac{\left(t_z + \frac{z_s}{h} + \frac{s}{2}\tan\phi\right)(\mu - \tan\phi) + \frac{C}{\gamma h}\frac{1}{\cos^2\phi}}{1 + \mu\tan\phi} \tag{24}$$

Equation (24) is a statement of the failure criterion of a buttress that fails in shear and needs to be compared with the elongation failure criterion given by Eq. (19). Contrary to Eq. (19) which does not involve any material parameters, the shear failure criterion given by Eq. (24) involves the coefficient of friction μ and the normalized

Author's personal copy

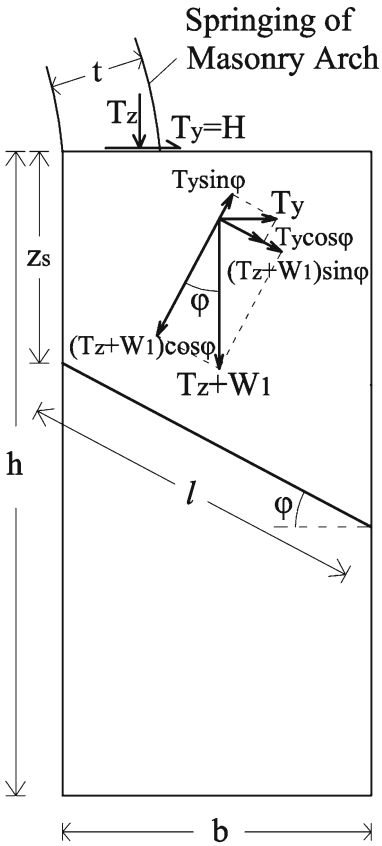


Fig. 6 Shear failure of a masonry buttress with coefficient of friction, μ, and cohesion force per length, C, along a failure plane inclined at an unknown angle, φ, due to an inclined force at its head with magnitude $\sqrt{T_y^2 + T_z^2}$

cohesion along the failure plane $C/(\gamma h)$. Values for the coefficient of internal friction of masonry range from $\mu = 0.5$ to $\mu = 0.7$ or even higher [11,24–28], while the cohesion of masonry assumes values of the order of $c = 150\,\text{kPa}$ or even lower given that even in the case where mortar has been used, this mortar will have been weak initially and will have decayed with time [9,25]. Denoting with, d, the out-of-the-paper dimension of the buttress ($c = C/d$), we adopt a specific weight, $\gamma/d = 22\,\text{kN/m}^3$. Accordingly, our dimensionless cohesion parameter $C/(\gamma h) = (C/d)/(\gamma h/d)$ assumes values of $C/(\gamma h) = 0.4$ and above (which occasionally may exceed unity), depending on the height, h, of the buttress.

Figure 7 plots the values of t_y offered by Eq. (24) as a function of the angle of the failure plane, φ, of buttresses with slenderness, $s = 0.2$ and 0.6, and coefficient of friction, $\mu = 0.7$. For each value of the slenderness, results for two values of the dimensionless cohesion are shown, $C/(\gamma h) = 0.5$ and 1.0, while in each plot, the dimensionless vertical force $t_z + z_s/h$ assumes values of $t_z + z_s/h = 0.25, 0.5, 0.75$ and 1. Figure 7 indicates that the limiting values of t_y associated with the admissible values of angle φ of the failure plane are finite and reach a minimum. Accordingly, among all physically admissible failure planes, the shear failure happens along the plane were t_y is minimum. Figure 7 further indicates that for the smaller value of the dimensionless cohesion (left plots, $C/(\gamma h) = 0.5$), the minimum value of t_y is associated with the higher possible value of $t_z + z_s/h$ and the angle of the failure plane is $\tan\varphi = 1.463 (t_y = 0.344)$ for $s = 0.2$ and $\tan\varphi = 2.271 (t_y = 0.169)$ for $s = 0.6$. Interestingly, as the value of the dimensionless cohesion increases, the values of t_y associated with the lowest value of $t_z + z_s/h$ become lower to the extent that for the case where $s = 0.2$ and $C/(\gamma h) = 1$, the value of $t_y = 0.970$ associated with a failure plane with $\tan\varphi = 0.477$ is comparable to the other minimum value of $t_y = 0.977$ associated with a failure plane with $\tan\varphi = 0.896$. Accordingly, in this case we may have a failure plane that passes by the -left corner of the buttress at an angle with $\tan\varphi \approx 0.48$.

Returning to the case where the cohesion is low enough so that the minimum value of t_y is associated with the higher value of $t_z + z_s/h$, the failure plane will pass by the bottom-right corner P of the buttress so that the maximum possible weight of the buttress is loading the failure plane. In this case,

Author's personal copy

$$\frac{z_s}{h} = 1 - s\tan\phi \tag{25}$$

Substitution of the expression given by Eq. (25) into Eq. (24) gives

$$t_y = \frac{\left(t_z + 1 - \frac{s}{2}\tan\phi\right)(\mu - \tan\phi) + \frac{C}{\gamma h}\frac{1}{\cos^2\phi}}{1 + \mu\tan\phi} \tag{26}$$

Equation (26) is the failure criterion in shear for a buttress with cohesion that is low enough so that the failure plane passes by the bottom-right corner, P, of the buttress. The angle φ of this failure is the angle which minimizes the normalized horizontal force, t_y, given by Eq. (26). Accordingly, the solution of the equation $\mathrm{d}t_y(\varphi)/\mathrm{d}\varphi = 0$ gives

$$\phi = \operatorname{arcsec}\sqrt{\frac{2\left(2\frac{C}{\gamma h}+s\right)\left[2\frac{C}{\gamma h}+s+(1+t_z)\,\mu\right](1+\mu^2) - 2\sqrt{\left(2\frac{C}{\gamma h}+s\right)^3\left[2\frac{C}{\gamma h}+s+2\,(1+t_z)\,\mu\right](1+\mu^2)}}{\left(2\frac{C}{\gamma h}+s\right)^2\mu^2}} \tag{27}$$

In Eq. (27), the values of the angle φ need to satisfy the constraint

$$0 \le \tan\phi \le \frac{1}{s} \tag{28}$$

so that the failure plane is within the buttress.

Figure 7 indicates that as the value of the dimensionless coherence, $C/(\gamma h)$, increases, the minimum value of t_y can be associated with the smaller possible value of $t_z + (z_s/h)$; therefore, in this case $z_s/h = 0$ and

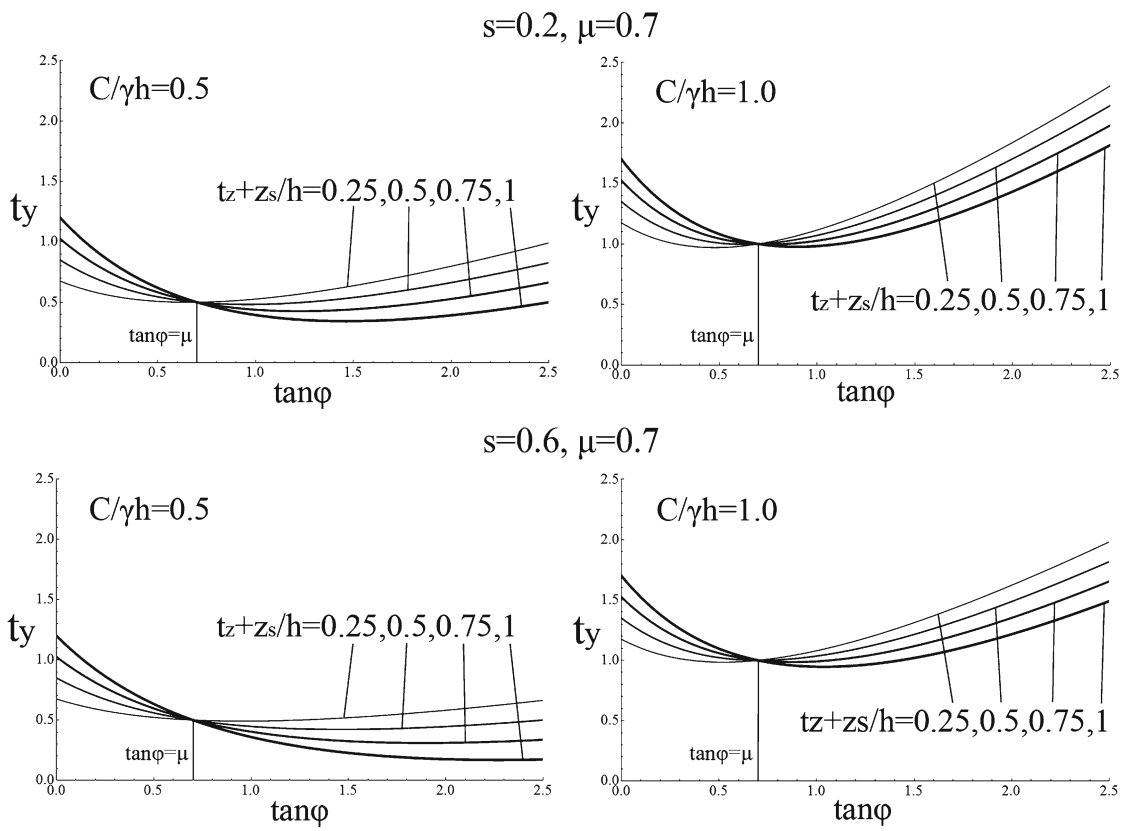


Fig. 7 Values of the normalized horizontal force, $t_y = T_y/(\gamma bh)$, offered by Eq. (24) as a function of the angle of the failure plane, φ, for various values of the normalized vertical load $t_z + z_s/h$

Author's personal copy

the angle of the failure plane passes by the upper-left corner of the buttress where the springing of the arch is meeting the buttress. In this case, the general equation for shear failure given by Eq. (24) simplifies to

$$t_y = \frac{\left(t_z + \frac{s}{2}\tan\phi\right)(\mu - \tan\phi) + \frac{C}{\gamma h}\frac{1}{\cos^2\phi}}{1 + \mu\tan\phi} \tag{29}$$

Equation (29) is the alternative failure criterion in shear for a buttress with cohesion that is large enough so that the failure plane passes by the upper-left corner of the buttress where the springing of the arch is meeting the buttress. The angle φ of this failure plane is the angle which minimizes the normalized horizontal force, t_y, given by Eq. (29). Accordingly, the solution of the equation $\mathrm{d}t_y(\varphi)/\mathrm{d}\varphi = 0$ gives

$$\phi = \arcsec\sqrt{\frac{2\left(2\frac{C}{\gamma h} - s\right)\left(2\frac{C}{\gamma h} - s + t_z\mu\right)(1+\mu^2) - 2\sqrt{\left(2\frac{C}{\gamma h} - s\right)^3\left(2\frac{C}{\gamma h} - s + 2t_z\mu\right)(1+\mu^2)}}{\left(2\frac{C}{\gamma h} - s\right)^2\mu^2}} \tag{30}$$

while the constraint of Eq. (28) needs to hold.

Figure 8 plots the critical values of the normalized horizontal force $t_y = T_y/(\gamma bh)$ as the cohesion of the buttress increases for three different values of the dimensionless vertical load $t_z = T_z/(\gamma bh) = 0.2$, 0.4 and 0.6. The solid line corresponds to a failure plane that passes by the bottom-right corner P, whereas the thin line corresponds to a failure plane that passes by the upper-left corner where the springing of the arch is meeting the buttress. For the lower values of the cohesion (say $C/(\gamma h) < 0.9$ for $t_z = 0.2$, $C/(\gamma h) < 1.25$ for $t_z = 0.4$ and $C/(\gamma h) < 1.5$ for $t_z = 0.6$), buttresses fail in shear by developing a failure plane that passes by the bottom-right corner P and only when the cohesion assumes larger values, the failure plane changes and passes by the upper-left corner. Figure 8 (lower plots) shows the tangent of the critical angle φ of the failure plane as the cohesion of the buttress increases. Figure 8 also shows that the normalized cohesion $C/(\gamma h)$ needs to be above a minimum threshold value for the masonry buttress to stand under gravity loads alone.

At this stage, we are in the position to establish the loading capacity of a masonry buttress by comparing the failure criterion in shear given by Eqs. (26) or (29) with the failure criterion in elongation given by Eq. (19). Figure 9 plots the values of the normalized horizontal force $t_y = T_y/(\gamma bh)$ as results from the above-mentioned failure criteria for three values of the dimensionless cohesion, $C/(\gamma h) = 0.4$, 0.6 and 0.8, and three values of the normalized vertical force $t_z = T_z/(\gamma bh)$ acting at the upper-left corner of the buttress.

The plots on the left of Fig. 9 show that when the normalized cohesion is relatively small ($C/(\gamma h) = 0.4$), a failure in shear becomes increasingly critical as the vertical load t_z increases. For instance, when $t_z = 0.4$ and $C/(\gamma h) = 0.4$, a buttress with slenderness up to $s = 0.2$ exhibits an elongation failure, whereas for $s > 0.2$,it exhibits a shear failure. When $t_z = 0.6$ (bottom-left plots), buttresses with any slenderness fail in shear.

6 Limit equilibrium analysis of a masonry tower subjected to lateral inertial loading

We are now interested in estimating the level of a constant ground acceleration that is capable of failing a masonry tower which exhibits zero tensile strength, sufficient compression strength and finite shear strength. The profile of a masonry tower may be either a slender rectangular, similar to that of the masonry buttress examined in the previous sections, or it may assume a tapered geometry as depicted in Fig. 10 which shows a view of a masonry chimney located in Piraeus, Greece.

Tall, slender structures have a tendency to flex, and as a result, the displacement profile increases with height. It is because of this "first mode" dominating response that the most popular equivalent static lateral force profile is that of an inverted triangle ([29], among others). At the same time, several of the tall chimneys have a tapered geometry; therefore, the distributed inertia mass decreases with height, while the displacement profile increases with height. In view of this combination of competing distributions, a uniform lateral equivalent static inertial loading may also be realistic [30]. Accordingly, in this paper we examine the failure mechanism of a tall rectangular masonry tower subjected to a uniform and a triangular distribution of lateral inertial forces.

Author's personal copy

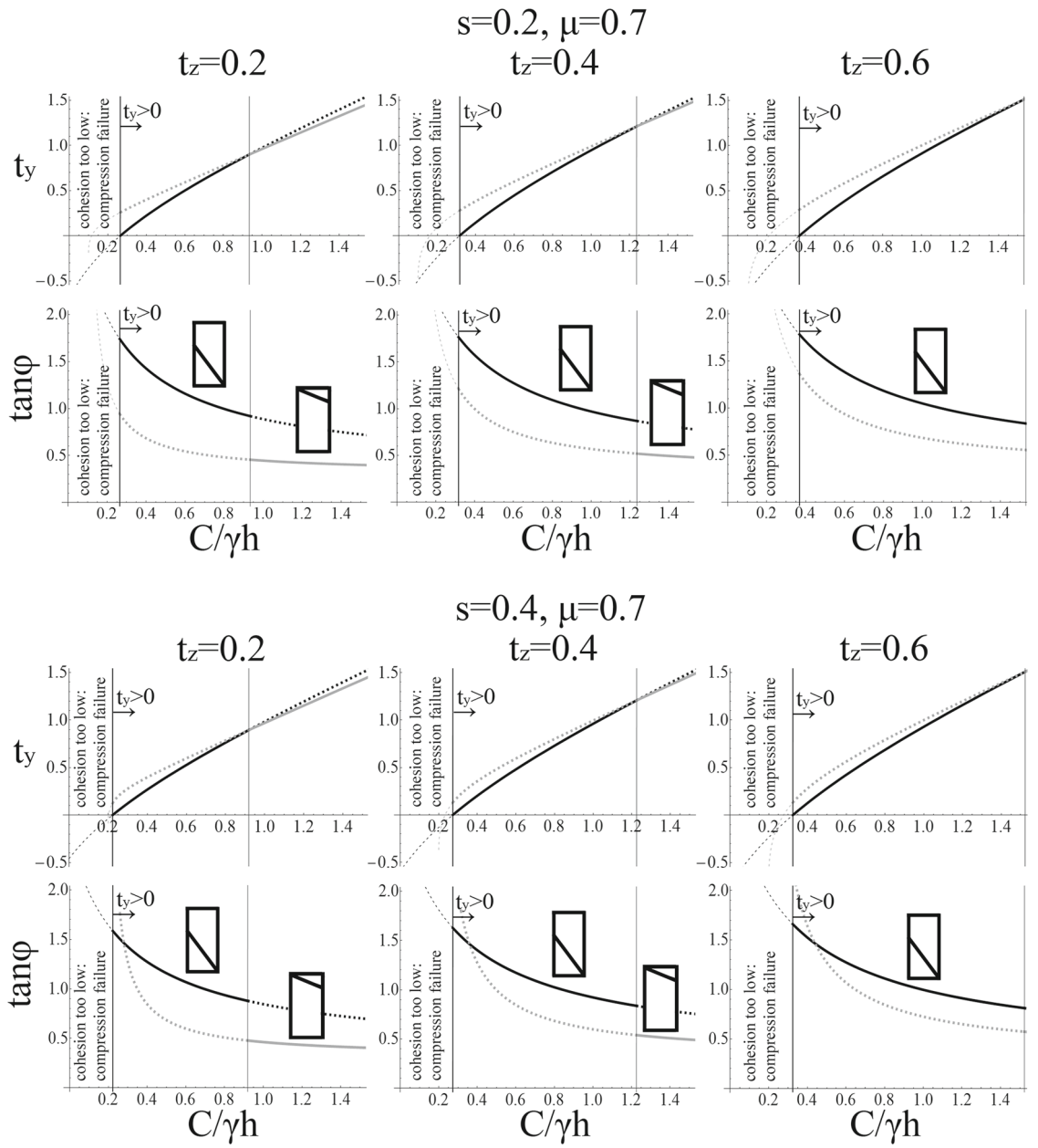


Fig. 8 Values of the critical lateral force $t_y = T_y/(\gamma bh)$ that is needed to fail in shear a buttress with slenderness $s = 0.2$ (*first row*) and $s = 0.4$ (*third row*) and $\mu = 0.7$ as its dimensionless cohesion $C/(\gamma h)$ increases. For the lower values of the cohesion, buttresses fail in shear by developing a failure plane that passes by the *bottom-right corner*, *P*, whereas for larger values of the cohesion, the failure plane changes and passes by the *upper-left corner* of the buttress. *Lower plots* Values of $\tan\varphi$ of the corresponding failure planes as the cohesion of the buttress increases

7 Thrust line of a masonry tower subjected to a uniform distribution of lateral inertia loading

With reference to Fig. 11, we consider a slender, rectangular masonry tower which in addition to its gravity load is subjected to a uniform lateral inertial loading, εg. Because of this equivalent static representation of the horizontal acceleration, εg, adopted in this analysis, the resultant acceleration field, $g = \sqrt{1+\varepsilon^2}$, is inclined at an angle ω from the vertical such that $\tan\omega = \varepsilon$. Consequently, the loading on a masonry tower subjected to a constant horizontal acceleration, εg, is equivalent to the gravity loading on the same tower when tilted at an angle $\omega = \tan^{-1}\varepsilon$ from the vertical. What is most interesting is that the elongation failure of an inclined slender tower under gravity loads alone has been examined by Heyman [9] more than two decades ago.

Author's personal copy

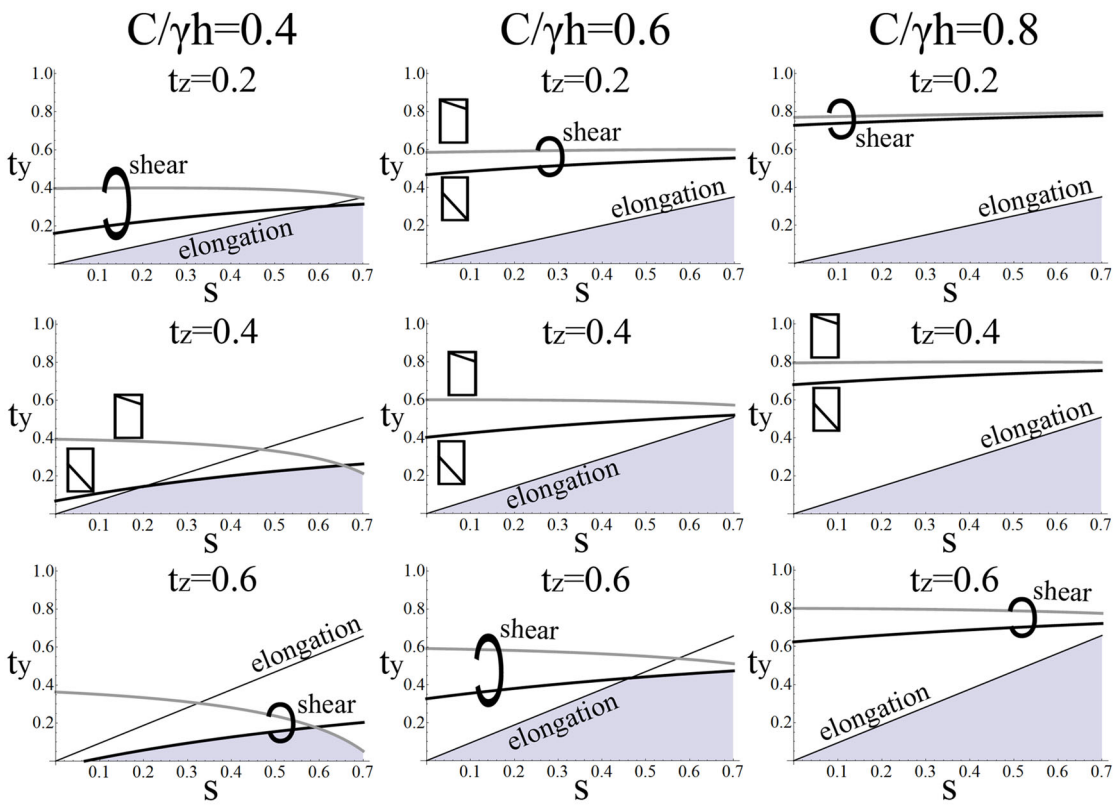


Fig. 9 Limiting normalized force $t_y = T_y/(\gamma bh)$ as results from elongation and shearing failure for three values of the dimensionless cohesion, $C/(\gamma h) = 0.4$, 0.6 and 0.8, and three values of the normalized vertical force $t_z = T_z/(\gamma bh)$ acting on the *upper-left corner* of the buttress. For the lower values of the cohesion, a failure in shear becomes increasingly critical as the vertical load t_z increases



Fig. 10 Views of one of the masonry chimneys located in Piraeus, Greece, in the neighborhood of Kaminia

Author's personal copy

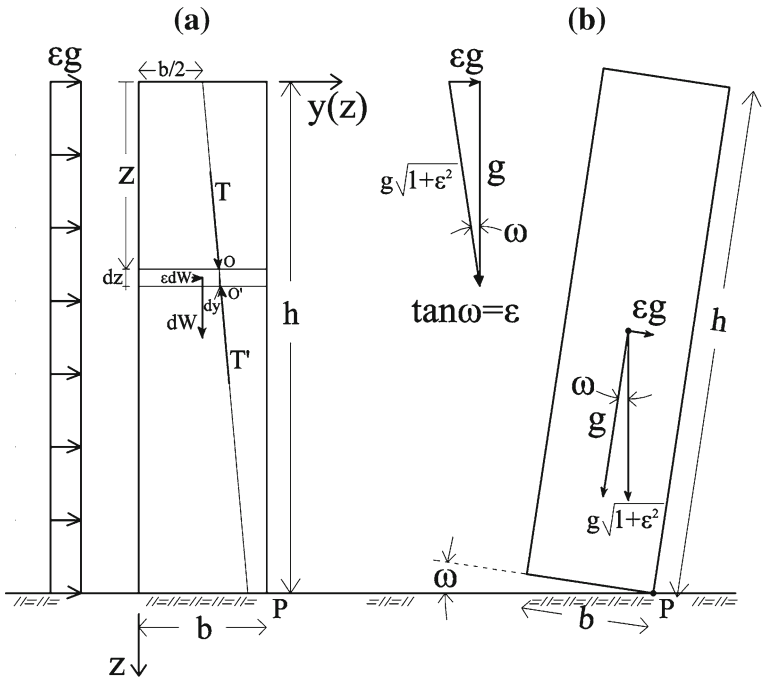


Fig. 11 Rectangular masonry tower subjected to a uniformly distributed inertia loading of intensity εg. The stress state of the leveled tower (*left*) subjected to its gravity load and a uniform distributed horizontal acceleration, εg, is equivalent to the stress state of a leaning tower by an angle of $\omega = \tan^{-1}\varepsilon$ (*right*) subjected solely to vertical forces—a problem that was analyzed by Heyman [9]

Before returning to the solution for the elongation failure of the tilted tower presented by Heyman [9], it is worth revisiting the equation of the thrust line that prevails in the tower prior to fracture. With reference to Fig. 11, the thrust line $y(z)$ initiates at half width at the top of the tower ($z = 0,\ y = b/2$) and evolves with a positive slope. The thrust line $y(z)$ is the geometrical locus of the application points of the resultant thrust forces acting at any horizontal cross section of the tower.

With reference to Fig. 11, let, T, be the thrust force at distance z and T' be the thrust force at distance $z + dz$ acting at point O'. Moment equilibrium of the elementary slice of the tower bdz about point O' gives

$$\gamma b z dy = \varepsilon \gamma b z dz - \gamma b dz \left(y(z) - \frac{b}{2} \right) \tag{31}$$

where γ is the surface force density of the tower ([Force]/[Length]^2). After rearranging terms Eq. (31) gives

$$z \frac{\mathrm{d}y(z)}{\mathrm{d}z} + y(z) = \varepsilon z + \frac{b}{2} \tag{32}$$

The solution of the linear differential Eq. (32) is

$$y(z) = \frac{A}{z} + \frac{\varepsilon}{2} z + \frac{b}{2} \tag{33}$$

where A is an integration constant which shall be zero ($A = 0$) given that at $z = 0$, $y(z = 0) =$ finite. Accordingly, the solution for the thrust line, $y(z)$, is a straight line

$$y(z) = \frac{\varepsilon}{2} z + \frac{b}{2} \tag{34}$$

From the equation of the thrust line given by Eq. (34), one can compute the level, ε, of the inertial loading that is capable of initiating a compression-free zone. By assuming a triangular stress distribution, the compression-free region originates at a distance z_e from the axis where the base of the triangular stress distribution is equal

Author's personal copy

to the width of the tower, b. At this distance, z_e, the resultant thrust force T_e is at a distance $y(z) = 2b/3$ and by virtue of Eq. (34), the compression-free zone starts at

$$z_e = \frac{b}{3\varepsilon} \tag{35}$$

Given that the result of Eq. (35) is meaningful only when $z_e \leq h$, we conclude that elongation fracture may initiate only when

$$\varepsilon > \frac{1}{3}\frac{b}{h} = \frac{1}{3}s \tag{36}$$

where $s = b/h$ is the slenderness of the tower.

8 Elongation failure of a masonry tower subjected to uniform lateral inertial loading

In view of the analogy between the stress state of (a) a vertical tower subjected to a uniform lateral inertial loading, εg, and (b) a tower leaning at an angle, $\omega = \tan^{-1}\varepsilon$, as illustrated in Fig. 11, the elongation fracture due to a uniform lateral inertial loading is precisely the parameterized solution $(f(t),\ z(t))$ presented by Heyman [9], where $\tan\omega$ is replaced by ε.

$$f(t) = b\left(1 - e^{1/4}2te^{-t^2}\right) \tag{37a}$$

$$z(t) = \frac{b}{3\varepsilon}\sqrt{\pi}e^{1/4}\left(\operatorname{erf}\left(\frac{1}{2}\right) - \operatorname{erf}(t)\right) \tag{37b}$$

where t is a parameter in the range $0 \leq t \leq 1/2$ [9]. For the facture line given by Eqs. (37a) and (37b), moment equilibrium of the convex fractured portion of the tower that tends to pivot about the pivoting point P at its base gives the level of lateral loading needed to induce uplifting [9]

$$\varepsilon = 0.7282s \tag{38}$$

where $s = b/h$ is the slenderness of the tower.

Equation (38) is a statement of the failure criterion of a masonry tower, with slenderness s, that fails in elongation when subjected to a uniformly distributed lateral load ε. Again, it is a failure criterion that does not contain any material parameters given that the analysis assumes that the joints of the masonry have zero tensile strength.

9 Shear failure of a masonry tower subjected to uniform lateral inertial loading

With reference to Fig. 12, we analyze the situation where the masonry tower fails in shear along a plane that is inclined at an angle φ. Assuming a trapezoidal failure, the weight of the upper portion of the tower is given by Eq. (21). Macroscopic force equilibrium parallel and normal to the failure plane gives

$$W_1 \cos\phi(\varepsilon + \tan\phi) = \mu N + C\frac{b}{\cos\phi} \tag{39}$$

$$N = W_1 \cos\phi(1 - \varepsilon\tan\phi) \tag{40}$$

The combination of Eqs. (21), (39) and (40) gives the level ε of the lateral inertial load capable of initiating sliding.

$$\varepsilon = \frac{\mu - \tan\phi + \frac{C}{\gamma h}\frac{1}{\cos^2\phi}\left(\frac{z_s}{h} + \frac{s}{2}\tan\phi\right)^{-1}}{1 + \mu\tan\phi} \tag{41}$$

Equation (41) offers the value ε of the uniform distributed lateral load that initiates sliding of an upper trapezoidal portion of the masonry tower along a plane inclined at an angle φ. The critical angle φ is the angle that minimizes the right-hand side of Eq. (41). At the same time, in order for the sliding plane to happen within the geometry of the tower

$$\frac{z_s}{h} \leq 1 - s\tan\phi \tag{42}$$

Author's personal copy

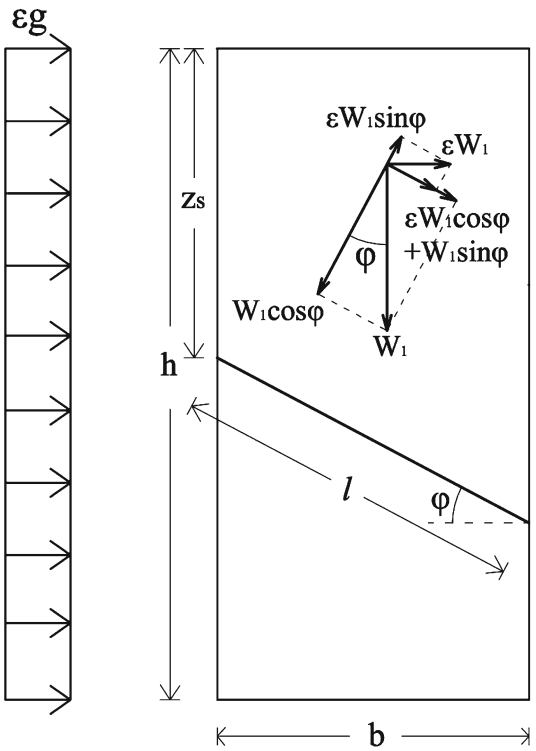


Fig. 12 Shear failure of a rectangular masonry tower with coefficient of friction, μ, and cohesion force per length, C, along a failure plane inclined at an unknown angle, φ, due to a uniform distributed inertia loading εg

Figure 13 plots the values of $\varepsilon(\varphi)$ offered by Eq. (41) as a function of the angle of the failure plane φ of a tower with slenderness, $s = 0.2$ and 0.6, and coefficient of friction, $\mu = 0.7$. For each value of slenderness, results for increasing values of z_s/h are shown, while satisfying the constraint given by Eq. (42). Figure 13 indicates that as z_s/h increases, the function $\varepsilon(\varphi)$ assumes lower values; nevertheless, the solution for $\varepsilon(\varphi)$ is arrested by the constraint given from Eq. (42). Accordingly, Fig. 13 indicates that the critical failure plane passes by the bottom-right corner of the rectangular tower; therefore,

$$\frac{z_s}{h} = 1 - s\tan\phi \tag{43}$$

Substitution of Eq. (43) into Eq. (41) gives

$$\varepsilon(\phi) = \frac{\mu - \tan\phi + \frac{C}{\gamma h}\frac{1}{\cos^2\phi}\left(1 - \frac{s}{2}\tan\phi\right)^{-1}}{1 + \mu\tan\phi} \tag{44}$$

In Eq. (44), the values of the angle φ need to satisfy the constraints of Eq. (28) so that the configuration of a trapezoidal failure holds. The critical values of $\varepsilon(\varphi)$ given by Eq. (44) are plotted in Fig. 13 with a heavy solid line which is merely the geometric locus of the end points of the curves, $\varepsilon(\varphi)$ given by Eq. (41). The minimum of the function $\varepsilon(\varphi)$ given by (44) corresponds to the critical values of ε and φ. The solution of the equation

$$\frac{\mathrm{d}\varepsilon(\phi)}{\mathrm{d}\phi} = 0 \tag{45}$$

is given by

$$\phi = \arcsec\sqrt{\frac{(4+s^2)(1+\mu^2)\left[8\left(\frac{C}{\gamma h}\right)^2 + \frac{C}{\gamma h}(6s+4\mu) + s^2(1+\mu^2)\right] - 4\sqrt{2}\sqrt{\frac{C}{\gamma h}(4+s^2)\left(2\frac{C}{\gamma h}+s+2\mu\right)(1+\mu^2)\left(2\frac{C}{\gamma h}+s+\frac{C}{\gamma h}s\mu+s\mu^2\right)^2}}{\left[2\frac{C}{\gamma h}(s-2\mu)+s^2(1+\mu^2)\right]^2}} \tag{46}$$

Author's personal copy

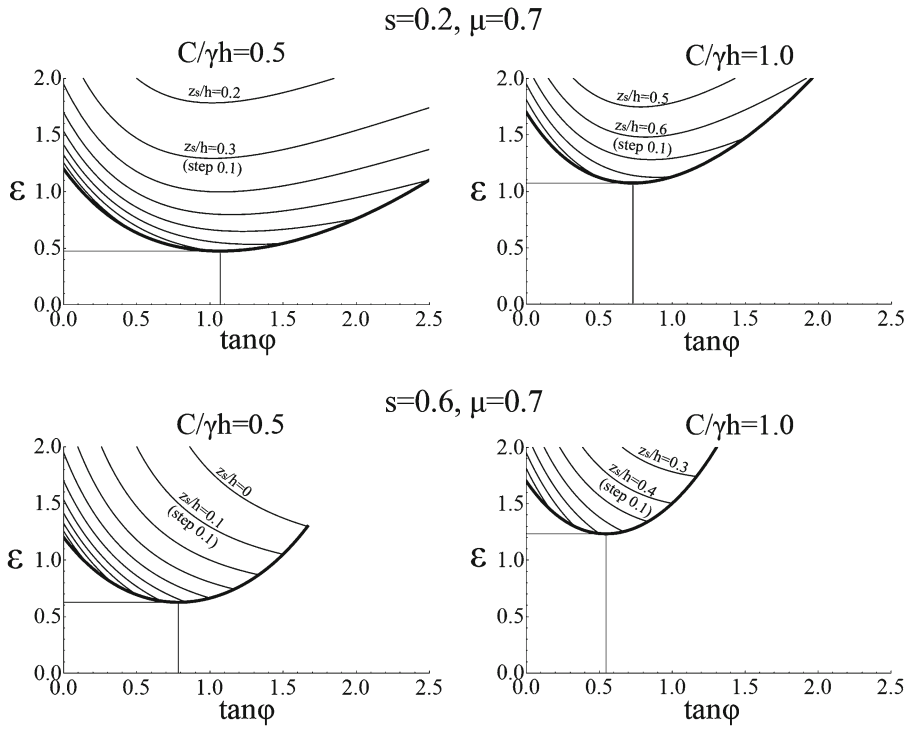


Fig. 13 Values of the lateral coefficient $\varepsilon(\varphi)$ offered by Eq. (41) as a function of the failure angle, φ, of a masonry tower with slenderness, $s = 0.2$ and 0.6, and coefficient of internal friction, $\mu = 0.7$. For each slenderness value, results for increasing values of z_s/h are shown, while satisfying the constraint $z_s/h \leq 1 - s\tan\varphi$ (*sliding plane* happens within the geometry of the tower)

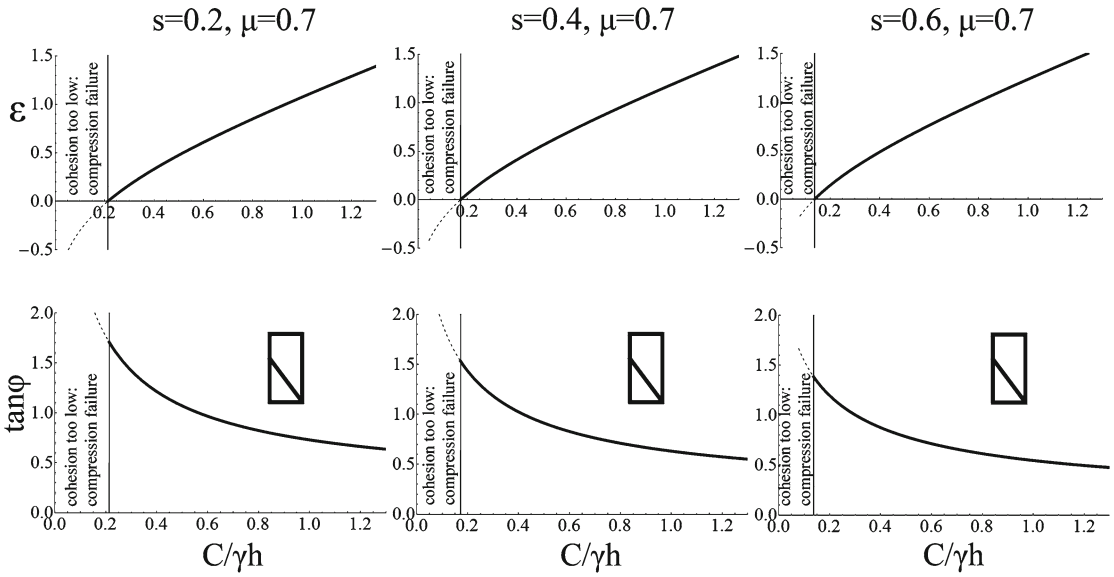


Fig. 14 *Top* Values of the critical seismic coefficient, ε, that is needed to fail in shear a masonry tower with slenderness $s = 0.2$, 0.4 and 0.6 as its dimensionless cohesion $C/(\gamma h)$ increases. *Bottom* Values of $\tan\varphi$ of the corresponding failure planes as the cohesion of the masonry tower increases. All failure planes pass by the *bottom corner* of the base

Figure 14 (top) plots the critical values of ε as the cohesion of the masonry tower increases for three different values of the slenderness, $s = 0.2$, 0.4 and 0.6. Figure 14 (bottom) shows the tangent of the critical angle φ of the failure plane as the cohesion of the buttress increases. Assuming a shear failure, the buttress fails by developing a shear failure plane that passes by the bottom corner of the base.

Author's personal copy

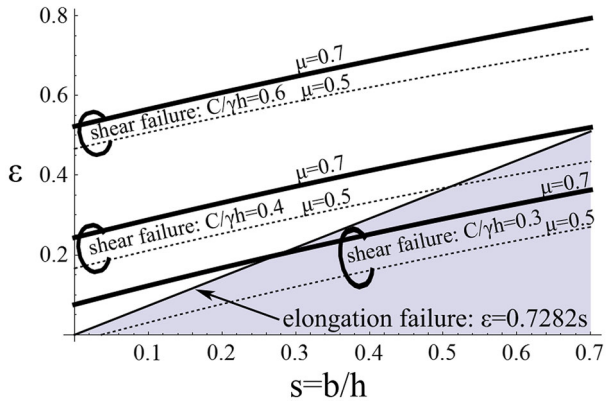


Fig. 15 Critical values of the seismic coefficient, ε, as a function of the slenderness of the masonry tower as they result from elongation and shear failure for two values of the coefficient of friction, μ, and three values of the dimensionless cohesion, $C/(\gamma h)$. For most practical cases, the elongation failure is the critical mode ($\varepsilon = 0.7282s$)

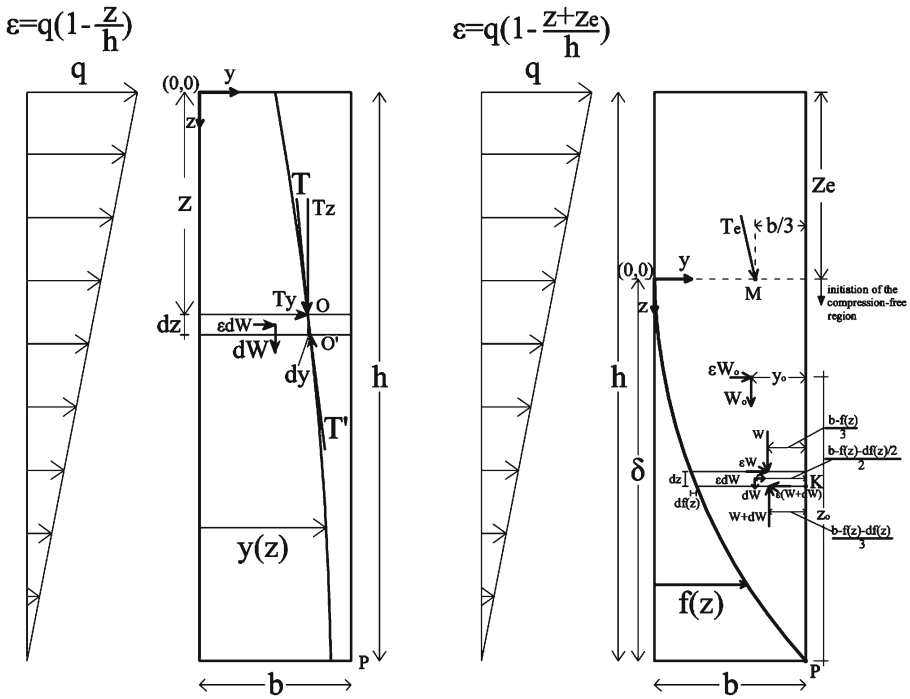


Fig. 16 *Left* Rectangular masonry tower subjected to an inverted triangular distribution of lateral inertial loading. The resulting *thrust line* on the tower is a parabola. *Right* Elongation failure of a masonry tower with surface density, γ, along the unknown curve $f(z)$ due to an inverted triangular distribution of lateral inertial loads

At this stage, we are in the position to establish the loading capacity of a masonry tower when subjected to a uniform distributed load by comparing the failure criterion in shear given by Eq. (44) with the failure criterion in elongation derived by Heyman [9] given by Eq. (38). Figure 15 plots the critical values of ε as they result from the above-mentioned failure criteria for two values of the coefficient of friction $\mu = 0.5$ and 0.7 and three values of the dimensionless cohesion, $C/(\gamma h) = 0.3$, 0.4 and 0.6. The plots show that under a uniform lateral distribution loading when the normalized cohesion is relatively small ($C/(\gamma h) = 0.3$—that is for a tall tower), a failure in shear may become critical. For higher values of the normalized cohesion (say $C/(\gamma h) \geq 0.4$), the elongation failure is in principle the critical failure mode.

Author's personal copy

10 Thrust line of a masonry tower subjected to a triangular distribution of lateral inertial loading

With reference to Fig. 16 (left), we now consider a slender rectangular masonry tower which in addition to its gravity load is subjected to a triangular distribution of lateral inertia loading that is zero at the base and assumes the value qg at the head of the tower. Under this loading configuration, the equation of the thrust line as a function of the independent variable z measured from the head of the tower is derived by taking moment equilibrium of an elementary slice of the tower bdz about point O'.
At any distance z from the tower's head, the horizontal load is

$$T_y = \gamma b \int_0^z q \left(1 - \frac{z}{h}\right) dz = \frac{1}{2}\gamma b q z \left(2 - \frac{z}{h}\right),$$

and moment equilibrium about point O' after dropping higher-order differentials gives:

$$\gamma b z dy - q\gamma \frac{b}{2} z \left(2 - \frac{z}{h}\right) dz + \gamma b dz \left(y - \frac{b}{2}\right) = 0 \tag{47}$$

where γ is again the surface density of the tower ([Force]/[Length]^2). After rearranging terms, Eq. (47) gives

$$z\frac{\mathrm{d}y(z)}{\mathrm{d}z} + y(z) = q\frac{z}{2}\left(2 - \frac{z}{h}\right) + \frac{b}{2} \tag{48}$$

The solution of Eq. (48) is

$$y(z) = \frac{A}{z} + q\frac{3h - z}{6h}z + \frac{b}{2} \tag{49}$$

where A is an integration constant which shall be zero ($A = 0$) given that at $z = 0$, $y(z = 0) =$ finite. Accordingly, the solution for the thrust line of a rectangular tower subjected to a triangular distribution of lateral loading is a parabola

$$y(z) = q\frac{3h - z}{6h}z + \frac{b}{2} \tag{50}$$

From the thrust line given by Eq. (50), one can compute the level of q that is capable of initiating a compression-free zone. By assuming a triangular stress distribution, the compression-free region originates at a distance z_e from the axis origin where the base of the triangular stress distribution is equal to the width of the tower b. At this distance, z_e, the resultant thrust force, T_e, is at a distance $y(z_e) = 2b/3$ and by virtue of Eq. (50), the compression-free zone starts at

$$z_e = \frac{h}{2}\left(3 - \sqrt{9 - 4\frac{s}{q}}\right) \tag{51}$$

Given that the result of Eq. (51) is meaningful only when $z_e \leq h$, we conclude that elongation fracture may initiate only when

$$q > \frac{1}{2}s \tag{52}$$

where $s = b/h$ is the slenderness of the tower.

11 Elongation failure of a masonry tower subjected to a triangular distribution of lateral inertial loading

With reference to Fig. 16 (right), the line of fracture $f(z)$ is the geometrical locus of the points in the masonry tower where the vertical compressive stresses vanish. Accordingly, the fracture line, $f(z)$, originates at a distance z_e from the head of the tower, where z_e is given by Eq. (51). In parallel to the previous analysis on the fracture of buttresses, the origin of the system of axis is translated down at $z = z_e$, so that the fracture initiates at $z = 0$. With this translation, the lateral load distribution is given by

$$\varepsilon(z) = q\left(1 - \frac{z + z_e}{h}\right) \tag{53}$$

Author's personal copy

At any location z of the fractured portion of the masonry tower, the resultant of the vertical forces, $W = W(z)$, is at a distance $(b - f(z))/3$ from the side of the tower that passes by the imminent pivot point P. With reference to Fig. 16 (right), moment equilibrium of the upper portion of the tower about point K gives

$$W(z)\frac{b-f(z)}{3} + dW(z)\frac{b-f(z)-\frac{df(z)}{2}}{2} = (W(z)+dW(z))\frac{b-f(z)-df(z)}{3} + q\left(1-\frac{z+z_e}{h}\right)W(z)dz \tag{54}$$

After eliminating higher-order differentials in association with Eqs. (10), (54) gives

$$W(z) = \frac{\gamma\,(b-f(z))^2}{2\left[3q\left(1-\frac{z+z_e}{h}\right)-\frac{\mathrm{d}f(z)}{\mathrm{d}z}\right]} \tag{55}$$

which upon differentiation

$$\frac{\mathrm{d}W(z)}{\mathrm{d}z} = \gamma\,(b-f(z))\,h\frac{3bq+6q(z+z_e-h)\frac{\mathrm{d}f(z)}{\mathrm{d}z}+2h\left(\frac{\mathrm{d}f(z)}{\mathrm{d}z}\right)^2+bh\frac{\mathrm{d}^2f(z)}{\mathrm{d}z^2}-f(z)\left(3q+h\frac{\mathrm{d}^2f(z)}{\mathrm{d}z^2}\right)}{2\left[h\frac{\mathrm{d}f(z)}{\mathrm{d}z}+3q(z+z_e-h)\right]^2} \tag{56}$$

After replacing the left-hand side of Eq. (56) with the result of Eqs. (10), (56) gives the differential equation that offers the fracture line $f(z)$

$$2\left[h\frac{\mathrm{d}f(z)}{\mathrm{d}z}+3q(z+z_e-h)\right]^2 - h\left[3bq+6q(z+z_e-h)\frac{\mathrm{d}f(z)}{\mathrm{d}z}+2h\left(\frac{\mathrm{d}f(z)}{\mathrm{d}z}\right)^2+bh\frac{\mathrm{d}^2f(z)}{\mathrm{d}z^2} - f(z)\left(3q+h\frac{\mathrm{d}^2f(z)}{\mathrm{d}z^2}\right)\right] = 0 \tag{57}$$

When the collapse mechanism is imminent, the line of fracture $f(z)$ will pass by the pivoting point, P; therefore, the boundary conditions of Eq. (57) are $f(0) = 0$ and $f(\delta) = b$, where $\delta = h - z_e$.

The challenge with the solution of the second-order nonlinear differential equation given by Eq. (57) is that the critical value of the lateral load, q, that is needed to initiate fracturing is also unknown. The second equation that is needed for solving this problem is that at the initiation of fracture, the detached portion of the tower satisfies moment equilibrium. Assuming that the masonry tower has fractured along the fracture line $f(z)$, moment equilibrium about the bottom corner P gives

$$q = \frac{\frac{b^2}{2}z_e + \frac{1}{2}\int_0^\delta (b-f(z))^2\,dz}{\frac{b}{2}z_e\left(2-\frac{z_e}{h}\right)\frac{h+\delta}{2} + \int_0^\delta (b-f(z))\left(1-\frac{z+z_e}{h}\right)dz\left[\delta - \frac{\int_0^\delta z(b-f(z))dz}{\int_0^\delta (b-f(z))dz}\right]} \tag{58}$$

where

$$\delta = h - z_e \tag{59}$$

The system of Eqs. given by (57), (58) and (59) is solved numerically, and the critical value of the lateral coefficient q is

$$q = 0.8884s \tag{60}$$

where $s = b/h$ is the slenderness of the tower.

Equation (60) is a statement of the failure criterion of a masonry tower with slenderness s that fails in elongation when subjected to a triangular distribution of lateral loads with peak value$= q$ at the tower head. Again, the failure criterion given by Eq. (60) does not contain any material parameters given that the analysis assumes that the joints of the masonry tower have zero tensile strength. Figure 21 indicates that the shape of the fracture line due to elongation failure is a curved line and the shape of the fractured portion of the tower that tends to pivot about the pivoting point P is slightly concave.

Author's personal copy

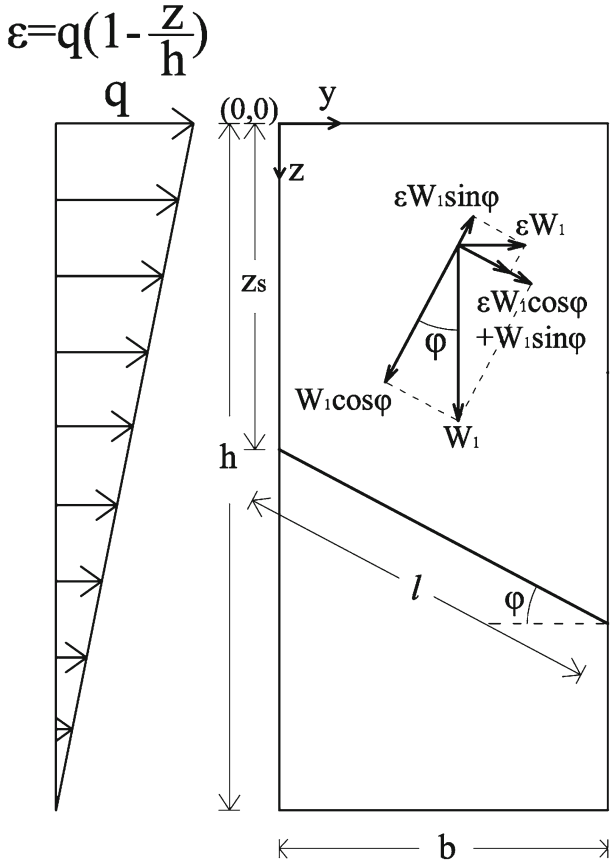


Fig. 17 Shear failure of a rectangular masonry tower with coefficient of friction, μ, and cohesion force per length, C, along a failure plane inclined at an unknown angle, φ, due to an inverted triangular distribution of lateral inertial loads

12 Shear failure of a masonry tower subjected to a triangular distribution of lateral inertial loading

With reference to Fig. 17, we now consider the situation where a masonry tower that is subjected to a triangular distributed load fails in shear along a plane that is inclined at an angle φ. Assuming a trapezoidal failure, the weight of the upper portion of the tower is given by Eq. (21) and macroscopic force equilibrium parallel and normal to the failure plane is expressed with Eqs. (39) and (40); where now

$$\varepsilon = \varepsilon(z) = q\left(1 - \frac{z}{h}\right) \tag{61}$$

The combination of Eqs. (21), (39), (40) and (61) gives the level of the coefficient q at the tower head capable of initiating sliding

$$q(\phi) = \frac{2\left(\frac{z_s}{h} + \frac{s}{2}\tan\phi\right)(\mu - \tan\phi) + 2\frac{C}{\gamma h}\frac{1}{\cos^2\phi}}{\left[\frac{z_s}{h}\left(2 - \frac{z_s}{h}\right) + s\tan\phi\left(1 - \frac{z_s}{h} - \frac{s}{3}\tan\phi\right)\right](1 + \mu\tan\phi)} \tag{62}$$

For the trapezoidal failure examined herein, Eq. (28) needs to hold.

Equation (62) offers the value of q at the tower head of an inverted triangular distribution of lateral loads that induce sliding of an upper trapezoidal portion of the masonry tower. The critical angle φ is the angle that minimizes the right-hand side of Eq. (62). At the same time, given that the sliding plane shall occur within the geometry of the tower, expression (42) also needs to hold. Figure 18 plots the values of $q(\varphi)$ offered by Eq. (62) as a function of the failure plane φ of a tower with slenderness $s = 0.2$ and 0.6 and coefficient of friction $\mu = 0.7$. For each value of slenderness, results for increasing values of z_s/h are shown, while satisfying the constraint given by Eq. (42). Figure 18 indicates that as z_s/h increases, the function $q(\varphi)$ assumes lower

Author's personal copy

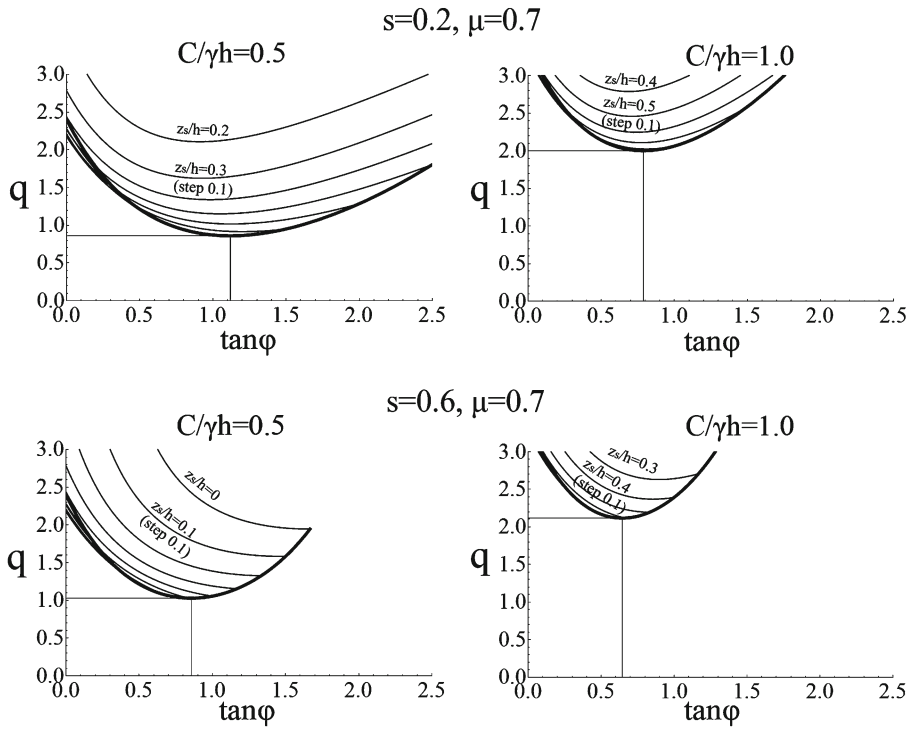


Fig. 18 Values of the lateral coefficient $q(\varphi)$ offered by Eq. (62) as a function of the failure angle, φ, of a masonry tower with slenderness, $s = 0.2$ and 0.6, and coefficient of internal friction, $\mu = 0.7$. For each slenderness value, results for increasing values of z_s/h are shown, while satisfying the constraint $z_s/h \leq 1 - s\tan\varphi$ (*sliding plane* happens within the geometry of the tower)

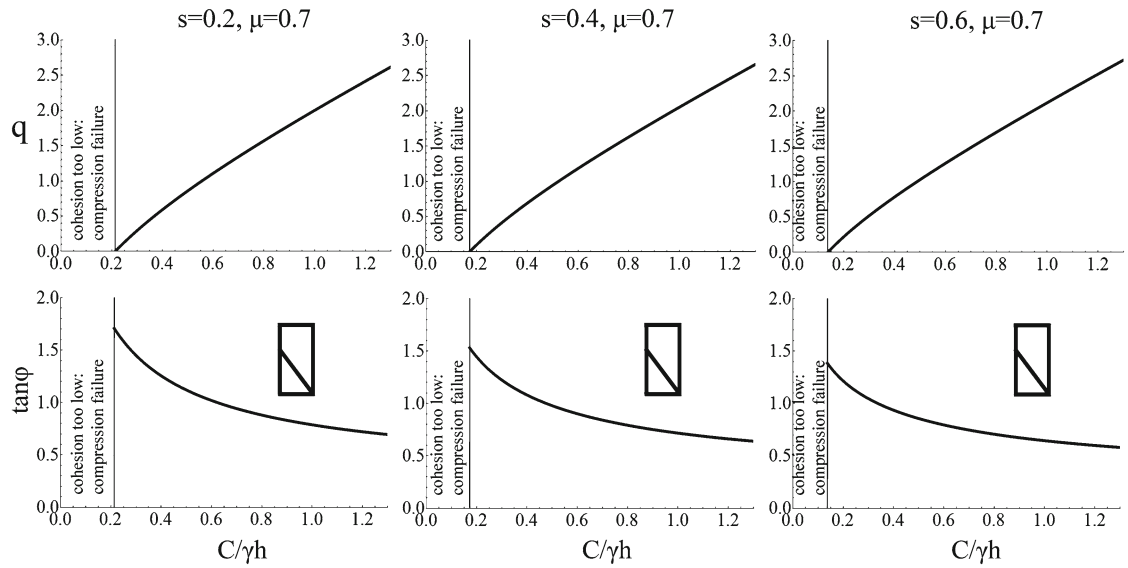


Fig. 19 *Top* Critical value of q that corresponds to the head of an inverted triangular distribution of lateral forces needed to fail in shear a masonry tower with slenderness, $s = 0.2$, 0.4 and 0.6 as its dimensionless cohesion $C/(\gamma h)$ increases. *Bottom* Values of $\tan\varphi$ of the corresponding failure planes as the cohesion of the masonry tower increases. All failure planes pass by the bottom corner of the base

values; therefore, the critical failure plane passes by the bottom-right corner of the rectangular tower. In this case, the height where the sliding initiates, z_s/h, and the angle of the sliding plane, φ, are related to Eq. (43). Substitution of Eq. (43) in Eq. (62) gives

Author's personal copy

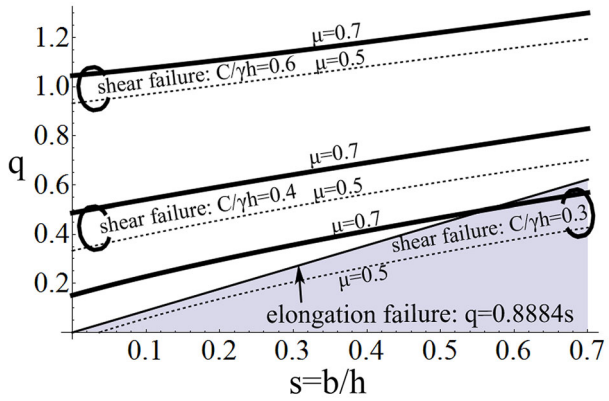


Fig. 20 Critical values of q that corresponds to the head value of an inverted triangular distribution of lateral forces as a function of the slenderness of the masonry tower as they result from elongation and shear failure for three values of the dimensionless cohesion, $C/(\gamma h)$. For most practical cases, the elongation failure is the critical mode ($q = 0.8884s$)

$$q(\phi) = \frac{2\left(1 - \frac{s}{2}\tan\phi\right)(\mu - \tan\phi) + 2\frac{C}{\gamma h}\frac{1}{\cos^2\phi}}{\left(1 - \frac{s^2}{3}\tan^2\phi\right)(1 + \mu\tan\phi)} \tag{63}$$

The values of $q(\varphi)$ given by Eq. (63) are plotted in Fig. 18 with a heavy solid line. The minimum of the function $q(\varphi)$ given by Eq. (63) corresponds to the critical values of ε and φ. The solution of the equation

$$\frac{\mathrm{d}q(\phi)}{\mathrm{d}\phi} = 0 \tag{64}$$

offers the exact value of the angle φ of the failure plane. Figure 19 (top) plots the critical values of q as the cohesion of the masonry tower increases for three different values of the slenderness, $s = 0.2$, 0.4 and 0.6. Figure 19 (bottom) shows the tangent of the critical angle φ of the failure plane as the cohesion of the masonry tower increases. Assuming a shear failure, the buttress fails by developing a failure plane that passes by the bottom corner of the base.

At this stage, we are in position to establish the lateral capacity of a masonry tower when subjected to a triangular distribution of lateral loads by comparing the failure criterion in shear given by Eq. (63) with the failure criterion in elongation given by Eq. (60). Figure 20 plots the critical values of q as a function of the slenderness, $s = b/h$, of the tower as they result from the above-mentioned failure criteria for three values of the dimensionless cohesion, $C/(\gamma h) = 0.3$, 0.4 and 0.6. As in the case of a uniform distributed load, the plots show that even when the normalized cohesion is relatively small ($C/(\gamma h) = 0.4$), a shear failure corresponds to a higher failure mechanism; therefore, under lateral inertial loading, the elongation failure is the a critical failure mode. Only when the dimensionless cohesion is very small (say $C/(\gamma h) = 0.3$) in association with a low value of a coefficient of friction ($\mu = 0.5$), a shear failure happens.

The findings of this study are summarized in Fig. 21, which shows the equations of the thrust line for the three different loading patterns (a: concentrated inclined force at the buttress head; b: uniform lateral inertial loading; and c: inverted triangular distribution of lateral inertial loading) together with the expressions of the critical loads according to the two failure mechanisms that were studied (elongation failure and shear failure).

13 A note on the seismic failure of masonry towers

The limit state analysis of tall masonry towers subjected to lateral seismic loads is treated in this work with an equivalent static procedure. The equivalent static lateral force procedure is a widely accepted procedure which is deeply rooted in most current seismic codes. Clearly, the results presented in Figs. 15 and 20 have technical merit and they indicate that a masonry tower, even with low cohesion along the joints of its stone when exited by lateral inertia loading will fracture in most cases due to an elongation failure.

Nevertheless, following the initiation of failure, the detached upper portion of the tower is about to enter a rocking motion by pivoting about the bottom corner P shown in Fig. 16. Given the dynamic nature of the loading, as the detached portion of the tower is about to enter rocking motion, the rotational (angular) acceleration to be developed engages the large rotational inertia of the detached portion of the tower [31–33].

Author's personal copy

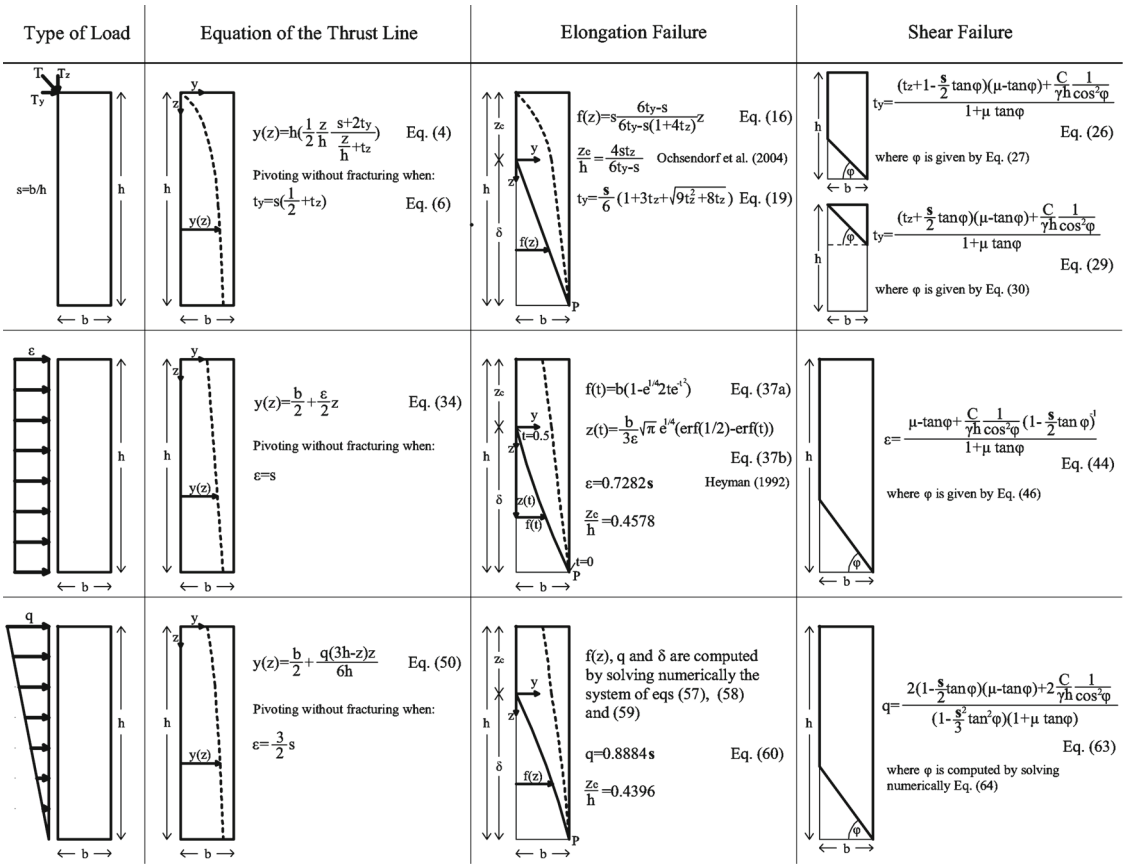


Fig. 21 Thrust lines, fracture lines and expressions of the critical loads according to elongation failure and shear failure of masonry buttresses and towers when subjected to three different loading patters

Accordingly, during the process of uplifting (still rotations are very small), the detached portion of the tower attracts additional inertial forces and by the time that the rotations are large enough to unlock the broken line of the elongation failure (see Fig. 5—top right), the inertial forces might be large enough to induce a follower shear failure. Accordingly, while this equivalent static analysis shows that under lateral inertial loading the elongation failure is a lower failure mechanism, the subsequent initiation of rocking that engages the large rotational inertia of the detached portion of the tower attracts additional inertia forces that may induce a follower shear failure. Accordingly, the collapse of a masonry tower may be the result of a combined elongation and shear failure.

14 Conclusions

This paper revisits the fracturing of masonry buttresses and towers when subjected either to a concentrated oblique force at their head or to lateral inertial loading due to ground shaking. Both a uniform and an inverted triangular distribution with height are examined. A concentrated oblique force at the buttress head usually results from the thrust that an elevated arch exerts on its supporting buttresses.

When a tall, slender masonry buttress with zero tensile, finite shear and sufficient compressive strength is subjected to a concentrated oblique force at its head, the buttress collapses in principle by developing an elongation fracture. Nevertheless, the paper shows that when the normalized cohesion along the stone joints of the buttress is small, a shear failure becomes increasingly critical as the vertical component of the inclined force at the head increases.

When a tall, slender masonry tower with zero tensile, finite shear and sufficient compressive strength is subjected to lateral, seismic inertial loading, a shear failure (except when the normalized cohesion is appreciably low) corresponds to a higher failure mechanism; therefore, under lateral inertial loading, the elongation failure is in principle the critical failure mode.

Author's personal copy

Given that the above results have been obtained with an equivalent static lateral force procedure, the paper explains that upon the elongation failure has occurred during the initiation of the process of rocking, the detached portion of the tower attract additional inertial forces due to the engagement of its large rotational inertia which may eventually induce a follower shear failure (before the detached portion of the masonry tower has experienced any noticeable rotations). Accordingly, the collapse of a masonry tower may be the result of a combined elongation and shear failure.

References

1. Audoy, M.: Mémoire sur la poussée des voûtes en berceau. Mémorial de l'officier du génie, no **4**, 1–96 (1820)
2. Dupuit, J.: Traité de l'équilibre des voûtes et de la construction des ponts en maçonnerie. Dunod Editeur, Paris (1870)
3. Heyman, J.: On the rubber vaults of the Middle Ages, and other matters. Gaz. des Beaux-Arts **71**, 177–188 (1968)
4. Heyman, J.: The Masonry Arch. Ellis Horwood, Chichester (1982)
5. Heyman, J.: The Stone Skeleton. Structural Engineering of Masonry Architecture. Cambridge University Press, New York (1995)
6. Sanabria, S.L.: The mechanization of design in the 16th century: the structural formulae of Rodrigo Gil de Hontañon. J. Soc. Archit. Hist. **41**, 281–293 (1982)
7. Huerta, S.: The Medieval 'scientia' of Structures: The Rules of Rodrigo Gil de Hontañón. Omaggio a Edoardo Benvenuto, University of Genoa, Italy (1999)
8. Huerta, S.: The safety of masonry buttresses. Proc. ICE Eng. Hist. Herit. **163**, 3–24 (2010). doi:10.1680/ehah.2010.163.1.3
9. Heyman, J.: Leaning Towers. Meccanica **27**, 153–159 (1992). doi:10.1007/978-94-017-2188-2_1
10. Ochsendorf, J.A., Hernando, J.I., Huerta, S.: Collapse of masonry buttresses. J. Archit. Eng. **10**, 88–97 (2004). doi:10.1061/(ASCE)1076-0431(2004)10:3(88)
11. Alexakis, H., Makris, N.: Structural stability and bearing capacity analysis of the tunnel-entrance to the stadium of ancient Nemea. Int. J. Archit. Herit. **7**, 673–692 (2013). doi:10.1080/15583058.2012.662262
12. Alexakis, H., Makris, N.: Minimum thickness of elliptical masonry arches. Acta Mech. **224**, 2977–2991 (2013). doi:10.1007/s00707-013-0906-2
13. Alexakis, H., Makris, N.: Limit equilibrium analysis and the minimum thickness of circular masonry arches to withstand lateral inertial loading. Arch. Appl. Mech. **84**, 757–772 (2014). doi:10.1007/s00419-014-0831-4
14. Alexakis, H., Makris, N.: Limit equilibrium analysis of masonry arches. Arch Appl. Mech. published on line (2014). doi:10.1007/s00419-014-0963-6
15. Makris, N., Alexakis, H.: The effect of stereotomy on the shape of the thrust-line and the minimum thickness of semicircular masonry arches. Arch Appl. Mech. **83**, 1511–1533 (2013). doi:10.1007/s00419-013-0763-4
16. Makris, N., Alexakis, H.: From Hooke's "hanging chain" and Milankovitch's "druckkurven" to a Variational Formulation: in Search of the Minimum Thickness of Masonry Arches. In: Proceedings of the 10th HSTAM International Congress on Mechanics, Chania, Crete, Greece, paper no. 2 (2013)
17. Makris, N., Alexakis, H.: The effect of stereotomy on the shape of the thrust-line and the minimum thickness of masonry arches. In: Proceedings of 9th International Masonry Conference, Guimarães, Portugal, paper no. 1461 (2014)
18. La Hire, P.: Sur la construction des voûtes dans les édifices. Mémoires de l'Académie Royale des Sciences, Paris (1731), pp. 69–77 (1712)
19. Bélidor, B.F.: La science des ingénieurs dans la conduite des travaux de fortification et d'architecture civile. C-A Jombert, Paris (1729)
20. Boothby, T.E.: Stability of masonry piers and arches including sliding. J. Eng. Mech. **120**, 304–319 (1994). doi:10.1061/(ASCE)0733-9399(1994)120:2(304)
21. Gilbert, M., Melbourne, C.: Rigid-block analysis of masonry structures. Struct. Eng. **72**, 356–361 (1994)
22. Ochsendorf, J.A., De Lorenzis, L.: Failure of rectangular masonry buttresses under concentrated loading. Proc. ICE Struct. Build. **161**, 265–275 (2008). doi:10.1680/stbu.2008.161.5.265
23. Coulomb, C.A.: Essai sur une application des règles des maximis et minimis à quelques problèmes de statique relatifs à l'arquitecture. Mémoires de mathématique et de physique, présentés à l'académie royal des sciences per divers savants et lus dans ses assemblées, Paris (1776) **7**, 343–382 (1773)
24. Rots, J.G.: Structural Masonry: An Experimental/Numerical Basis for Practical Design Rules. A.A. Balkema, Rotterdam (1997)
25. Macorini, L., Izzuddin, B.A.: A non-linear interface element for 3D mesoscale analysis of brick-masonry structures. Int. J. Numer. Methods Eng. **85**, 1584–1608 (2011). doi:10.1002/nme.3046
26. Konstantinidis, D., Makris, N.: Seismic response analysis of multidrum classical columns. Earth Eng. Struct. Dyn. **34**, 1243–1270 (2005). doi:10.1002/eqe.478
27. Konstantinidis, D., Makris, N.: Earthquake analysis of multidrum columns. In: 5th International Conference on Earthquake Resistant Engineering Structures (ERES 2005), Skiathos, Greece (2005)
28. Alexakis, H., Makris, N.: Stability analysis of the underground masonry tunnel of Ancient Nemea. In: Bilotta, E., Flora, A., Lirer, S., Viggiani, C. (eds.) Geotechnical Engineering for the Preservation of Monuments and Historic Sites. CRC Press, Taylor & Francis Group, London (2013)
29. Clough, R.W., Penzien, J.: Dynamics of Structures, 2nd edn. McGraw-Hill, New York (1993)
30. DeJong, M.J., Vibert, C.: Seismic response of stone masonry spires: computational and experimental modeling. Eng. Struct. **40**, 566–574 (2012). doi:10.1016/j.engstruct.2012.03.001

Author's personal copy

31. Makris, N.: The role of the rotational inertia on the seismic resistance of free-standing rocking columns and articulated frames. Bull. Seismol. Soc. Am. **104**, 2226–2239 (2014). doi:10.1785/0120130064
32. Makris, N.: A Half-Century of Rocking Isolation. Earthquakes and Structures, 7, published online (2014). doi:10.12989/eas.2014.7.6.000
33. Makris, N., Vassiliou, M.F.: The dynamics of the rocking frame. In: Psycharis, I.N., Pantazopoulou, S.J., Papadrakakis, M. (eds.) Seismic Assessment, Behavior and Retrofit of Heritage Buildings and Monuments. Computational Methods in Applied Sciences. Springer International Publishing, Switzerland (2015). doi:10.1007/978-3-319-16130-3XXUndXX2